Borneo Akademika *Vol. 4 Special Issue October 2020*, 42 - 58
UiTM Cawangan Sabah

EFFECT OF FOREARM ROTATION TOWARDS CROSS-USER CLASSIFICATION ACCURACY OF FOREARM GESTURES

(Kesan Putaran Lengan Terhadap Kejituan Pengkelasan Gerak Isyarat Merentas Pengguna)

ZINVI FU[1*], AHMAD YUSAIRI BANI HASHIM[2], ZAMBERI JAMALUDIN[2], & IMRAN SYAKIR MOHAMAD[2][1]Department of Mechanical Engineering, Politeknik Kota Kinabalu, Sabah
[2]Faculty of Manufacturing Engineering, Universiti Teknikal Malaysia, Melaka

zinvifu@polikk.edu.my

ABSTRACT

Electromyography (EMG) is a random biological signal that depends on the electrode placement and the physiology of the individual. Currently, EMG control is practically limited by this individualistic nature and requires per session training. This study investigates the EMG signals based on six locations on the lower forearm during contraction. Gesture classification was performed en-bloc across 20 subjects without retraining with the objective of determining the most classifiable gestures based on the similarity of their resultant EMG signals. Principle component analysis (PCA) and linear discriminant analysis (LDA) were the principal tools for analysis. The results showed that many gesture pairs could be accurately classified per channel with accuracies of over 85%. However, classification rates dropped to unreliable levels when up to nine gestures were classified over the single channels. The classification results show universal classification based on a common EMG database is possible without retraining for limited gestures.

Keywords: Electromyography, user-independent, rotation-independent, hand exchange independent, classification, principal component analysis, linear discriminant analysis

1. Introduction

The electromyogram (EMG) is the electrical activity produced at the skeletal muscle during contraction. With the appropriate electrodes and amplification, it can be detected and used for a broad scope of studies, including medical diagnostics, biomechanics, and the design and applications of prosthetics and human-machine interfaces (Mane, Kambli, Kazi, & Singh, 2015). Being a biological signal, the nature of the EMG signal is user specific. The EMG signal for machine control is typically processed in two stages: first, feature extraction, which serves to reduce the dimensionality of the signal; followed by classification, a prediction algorithm. These data processing is performed on computers or embedded systems. Prior to prediction, the classifier is first trained multiple times with features from a signal. Once the classifier has enough known content to establish class membership, unknown content can be accurately evaluated if it belongs to the class or not. Obviously, the accuracy of the predicted class (in this case, hand gestures) depends on the consistency of the training data and the distinction from the test data pattern.

On the application of machine control, EMG machine control remains a novelty and has not seen widespread practical applications in spite of the numerous studies, as highlighted by Artemiadis (2012) and Jiang, Dosen, Muller, & Farina Jiang et al (2012).

1. Practical EMG issues: user, hand position and arm exchange independence

In many reports, the EMG as a machine input signal shows promising results: achieving a classifier accuracy of over 90 %. It is well established that a classifier can perform well when trained on subject subject-specific cases, as shown by Watts et al*et al*. (2008) and Souissi, Zory, Bredin, & Gerus Souissi et al. (2017). In additionNonetheless, the EMG classifier wiloulld usually require retraining on each session, even when applied on the same subject (Liu, Zhang, Jiang, & Zhu, 2015; Phinyomark et al*et al*., 2013) (Phinyomark et al., 2013), (Liu, Sheng, Zhang, Jiang, & Zhu, 2016). On multi-user classification, Kerber, Puhl, & Krüger Kerber et al. (2017) worked towards classifying up to 40 gestures with a combination of up to10 extracted features from 14 users. In their work, Aa common classifier was trained with data from all 14 subjects. The classification accuracy was obtained at 97% withfor 5five gestures and down to 16 % when attempting to classify all 40 signals. Therefore, an accuracy of about 70 % is a reasonablyrealistic performance good for a nine-class classification, as ascertained by Piskorowski.(2013).

The forearm is a highly articulated limb, capable of many different gestures. However, as shown by Leijnse, Campbell-Kyureghyan, Spektor, & Quesada Leijnse (2008), most of the EMG recordings have to be made with the arm constrained to specific positions. This is because the slightest wrist rotation (pronation and supination) will produce distinctively different EMG signals (Yung & Wells, 2013). In addition, Saponas et al*et al*. (2009) demonstrated that the EMG changes as the forearm rotates. On the same matter, Yang, Yang, Huang, & Liu Yang et al. (2017) and Geng, Zhou, & LiGeng et al. (2012) have also shown that the misclassification of forearm signals correlates to wrist rotation rather than hand position.

In response to the problems posed by the varying EMG signal due to wrist rotation, Xu et al*et al*. (2011), Stival, Michieletto, & Pagello Stival et al. (2016), and Fougner, Scheme, Chan, Englehart, & Stavdahl Fougner et al. (2011) showed that the rotation independence could be improved by using EMG in conjunction with accelerometers. Their methods effectively reduced classification error from 18% to 5%.

On hand-exchange, Kim, Mastnik, & André Kim et al. (2008) noted a negligible difference in the EMG of the left and right hand. However, in a later in-depth study, Khushaba (2014) has proven otherwise - the data field of the opposite hands are fairly different.

2. Towards zero-retraining

Training is necessary in almost every recorded work (Cai et al*et al*., 2019; Sensinger, Lock, & Kuiken, 2009) (Sensinger, Lock, & Kuiken, 2009), (Cai et al., 2019). The purpose of training in simple terms is to allow a classifier to learn variations of a class. The classifier then estimates the class membership of the fresh data (test data) by comparing it against historical data (training data). Training time can range between 10 to 30 minutes (Shenoy, Miller, Crawford, & Rao, 2008; Stoica et al*et al*., 2012) (Shenoy, Miller, Crawford, & Rao, 2008) to 30 minutes (Stoica et al., 2012). Some works have tried to address the issue, by proposing methods to accommodate a small training data set (Sun & Chen, 2012), and even eliminating the training session (Liu, Zhang, Jiang, & Zhu, 2015). However, Phinyomark et al*et al*. (2013) reported that

classification accuracy dropsped when retraining is not performed. Therefore, classification accuracy is also a measure of the retraining scheme and cannot be entirely disregarded.
In recent years, there has been some interest in eliminating retraining. Huang, Zhang, Sun, & He Huang et al. (2010) and Liu et al*et al*. (2015) introduced methods that provided reliable classification without retraining. On the other hand, Phinyomark (2013) showed a novel sample entropy feature with LDA classification could reduce the gap of zero retraining by a margin of 2.5%. However, these methods were performed with limited subjects. wWith the introduction of cross user non-retraining, Stival et al*et al*. (2016) obtained mixed results in classification accuracy. In conclusion, these works show that common data exists between individuals, despite the various physiological differences.

3. Problem statement and objective of the study

In practical applications, the device may be used by various individuals at different hand positions. Per-session training, although essential, is not practically viable. Since the possibility of zero-retraining was implied, this study aims to study the gap between the accuracy and practicality of cross-subject hand gesture classification in lieu of classifier retraining.
This study aims to determine the effect of hand rotation towards the classification accuracy of hand gestures in the influence of multiple users. The results would suggest the best classifiable gestures, which are not only compatible across various individuals, but also robust towards arm rotation.

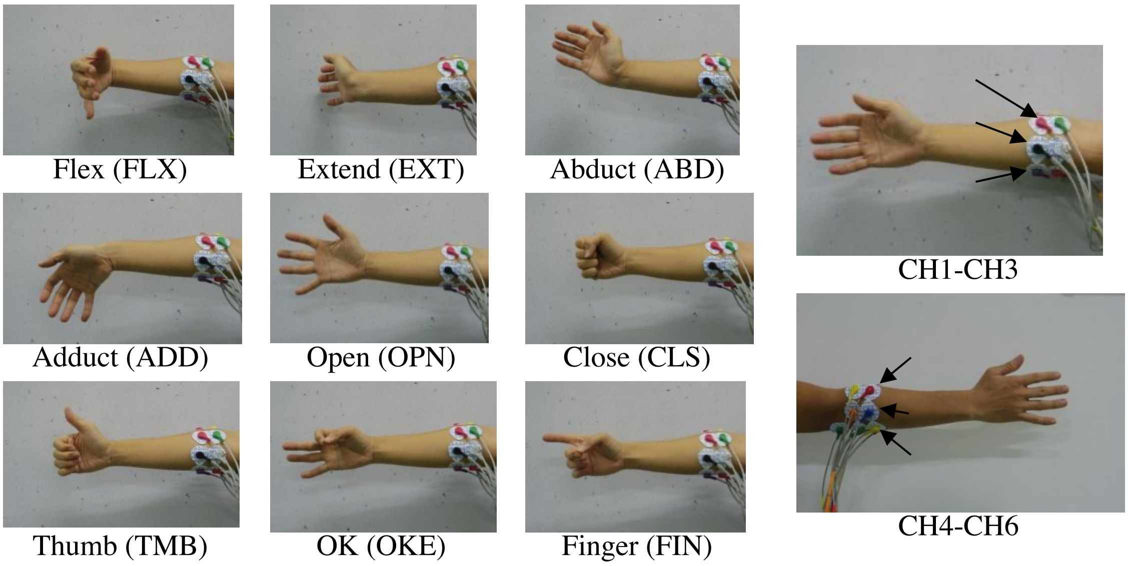

Figure 1: Gestures performed for classification. There are six wrist gestures: FLX, EXT, ABD, ADD, OPN and CLS; and three three-finger gestures: FIN, TMB, and OKE. The gestures were recorded in sequence with the arm down in natural position.

2. Research Questions

1. To study the classification accuracy of hand gestures over a multi-subject data field in a realistic environment, the following research questions have been established:

2. In a multi-subject session, by how far does the forearm rotation affect classification accuracy?

3. In the influence of wrist rotation, which gestures is the most easily classifiable (highest classification accuracy)?

3. Methodology

1. Subject Demographics and Equipment

Twenty right-handed subjects, consisting of 10 males and 10 females participated in the study. The subject's demography ranges from age 24-42 with a mean age of 30. The BMI of the subjects ranged from 15 to 32 with a mean of 23, with 55% having a normal BMI class. No movement restriction or pain associated with the wrist and finger were reported. However, two subjects, one male and female, reported to have having mild essential tremor. All subjects voluntarily gave written informed consent to participate in the experiment.

The EMG amplifier was designed specifically for this experiment. The design, which was based on the INA121P instrumentation amplifier has an effective CMRR of 78.64 dB and adjustable gain of 250. Pre-processing methods incorporated into the design consisted of a bandpass filter with a range of 18.97 Hz to 709 Hz. More details on our design can be found in (Fu, Bani Hashim, Jamaludin, & Mohamad, 2016) and (Fu, Bani Hashim, Jamaludin, Mohamad, & Nasir, 2017). The data was acquired with the National Instruments NI-cDAQ 9178 data acquisition unit (DAC) with the NI9205 input module, sampled at 5 kHz and LabVIEW as the user interface. Post-processing was done with the Matlab 2010 software.

Six pairs of Ag-Cl wet electrodes were placed with equal distance around the lower forearm, at about 30 mm below the elbow. An additional reference electrode was attached to the elbow. A shielded cable was used to connect the EMG amplifier to the electrodes. With the arm at neutral position, placing began with CH1 placed directly below the elbow, on the posterior side of the forearm. The other channels are then placed at $d_e = \times$ circumference. With the electrodes placed, the electrodes were connected to the EMG amplifier with shielded cables.

The subjects performed the nine gestures, in a sequence flex (FLX), extend (EXT), abduct (ABD), adduct (ADD), open (OPN), close (CLS), finger (FIN), OK (OKE) and thumb (TMB), as shown in Figure 1. The gestures were performed with the left hand (LH) in neutral position (DN), followed by wrist pronation (DP) and supination (DS). The procedure was repeated on the right hand (RH).

The EMG data from the gestures were then classified individual channels in two cases: pair-wise gesture per channel, and all gestures per channel. In both cases, the classification accuracy of the gestures in DN position was compared to that of the DP and DS position.

2. *Data reduction and gesture classification*

Prior to analysis, signal conditioning was performed unto on the EMG waveforms done to eliminate transient conditions. Rectification followed by a 10 Hz linear envelope feature extraction. Next, the stochastic EMG signal was smoothened and simplified to results comparable to moving average (MAV), and root mean square (RMS) features. The reduced waveform would be more efficient for post-processing. The repetitive time-varying dimension is further reduced with principal component analysis (PCA), which effectively reduces the dimensionality of the dataset.

The PCA is an orthogonal linear transformation that decorrelates the multivariate data and projects it onto a new coordinate system, where the greatest variance lies on the first axis, followed by the next greatest variance on the following axis. If a vector, *z* of length N has M observations, then the PCA transform is performed first by subtracting the mean from the vector

$$\bar{x} = \bar{z} - E[z] \quad (1)$$

The covariance matrix *C* is defined as

$$C = E[\bar{x}\bar{x}'] \quad (2)$$

The principle components, PC of $\bar{x}$, are defined in terms of the unit-length eigenvectors ($\bar{e}_1, \bar{e}_2, \ldots \bar{e}_n$) of C, giving

$$\bar{s} = W\bar{x} \quad (3)$$

The projection matrix, *W* contains the eigenvectors ($\bar{e}_1, \bar{e}_2, \ldots \bar{e}_n$). The *M* observations are normally exemplars taken from any one of the *C* classes.

The dataset representing all gestures performed in all states of the arm is stored in a six-dimension matrix in the order of subject, channels:

$$D = \{ D_{S1\text{-}S20}, D_{LH\text{-}RH}, D_{P,N,S}, D_{G1\text{-}G20}, D_{CH1\text{-}CH6} \}. \quad (4)$$

The result of the PCA dimensionality reduction can be plotted to show separation of the gestures. The PCA representation can be easily separated with from Linear discriminant analysis (LDA), a powerful method for classifying EMG patterns (Phinyomark, 2013).

The LDA is a supervised classifier, whereby classes must be pre-defined before training is done. LDA works on the principles of Baye's Theorem, which estimates the probability of the data belonging to each class. With the input class as *x(k),* the probability of the output class (k) is given by,

$$P(Y=x|X=x) = \frac{(PI_k.fk(x))}{\sum (PI_l.fl(x))}$$

PI_k refers to the base probability of each class (k) observed in the training data, defined as:

$$PI_k = \frac{nk}{n}$$

The LDA assumes the probability of x belonging to a class is, f(x) is Gaussian. Therefore, the discriminant function *Dk(x)* is given as:

$$Dk(x) = x\left(\frac{\mu k}{\sigma^2}\right) - \left(\frac{\mu k}{2\sigma^2}\right) + \ln(PI_k)$$

Dk(x) is the discriminate function for class *k*, given input *x*.

Classification was performed on two gesture classes per channel. Therefore, all possible gesture pairs e.g., FLX-EXT, FLX-ABD FLX-ADD were iterated and individually classified across the six channels. The classification was repeated on every state: LH, RH, DN, DP, DS. The effect of rotation (pronation and supination) of the forearm towards the classification accuracy serves as a measure of how robust the gesture is towards forearm rotation.

4. Results and Discussion

A sample of the acquired raw EMG waveform is shown in Figure 2 (a). The gestures were performed in a sequence that lasted about 30 seconds, which each gesture typically about 1.5 seconds long. The dynamics of the EMG output varies over the channels. For instance, the FLX gesture is more significant in CH3 and CH4 as opposed to other channels, indicating that these channels may be more useful for classifying these gestures. CH1 and CH2 also display less dynamics compared to other channels. Some ECG contamination can be observed in CH5. The frequency response is shown in Figure 2 (b) indicates that the bulk of the EMG activity lies at the 100 Hz region. A 10 Hz linear envelope shown in Figure 2 (c) was applied to shape the EMG waveform. As shown hereIn general, 10 Hz is sufficient to retain the transient shape of the waveform. For each hand per subject, there were 27 gestures (9 gestures x 3 position).

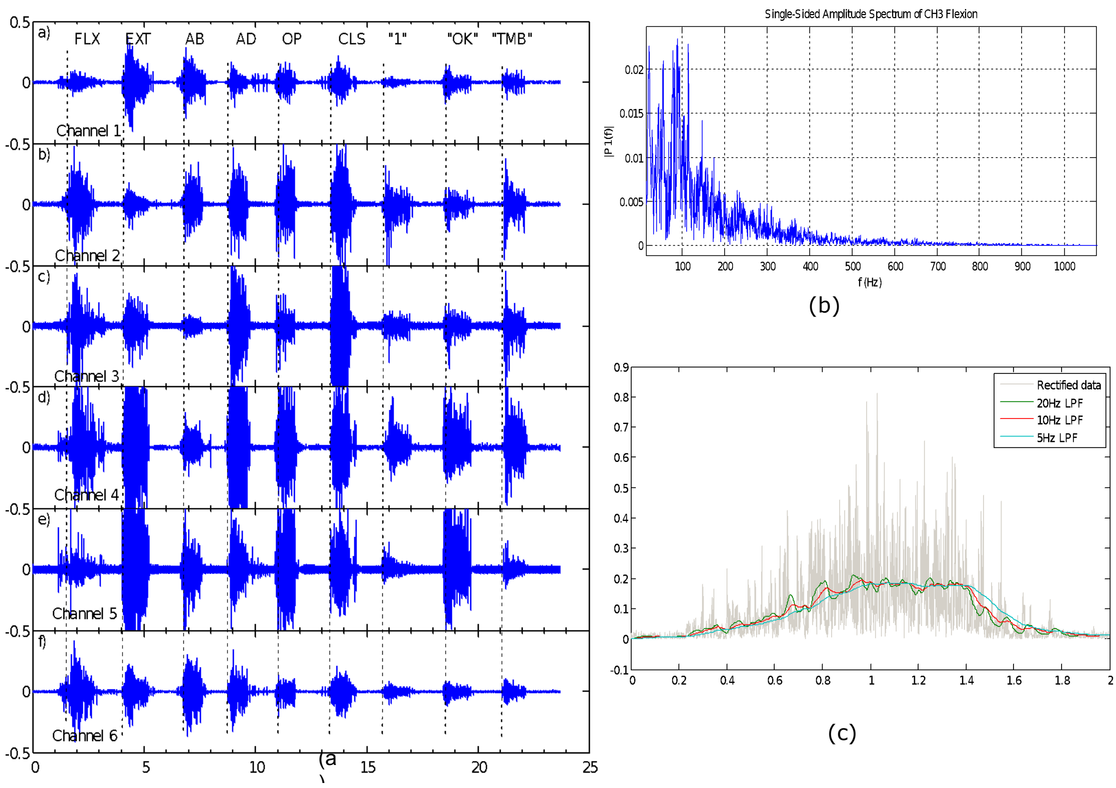

Figure 2: The rectified waveform (grey) is filtered with a 2nd order low pass filter. Shown

are the effects of a 20Hz, 10Hz and 5 Hz filter.

1. Results of PCA dimensionality reduction

The results of the PCA dimensionality reduction is shown in Figure 3. The centroid of the gesture, which represents the mean signal of the 20 subjects and its standard deviation (STD) is shown in Figure 3. The size of the circular perimeter indicates the similarity of the EMG wave of the gesture. To provide the grounds for good classification, each gesture points should be well separated with a small STD radius. If the pronation, supination and neutral markers are in place, it shows that the channel-gesture is resistant to wrist rotation.

For the plot, the three markers (triangle, star, and circle) represent a gesture in neutral, pronation, and supination. The shapes represent the state of the forearm rotation: circle for neutral, star for pronated and triangle for supinated. Ideally, the markers of the gestures in all three forearm positions should be at the same location, with the smallest radius. The wider distance between these markers indicates pattern shift due to rotation. For the left-hand sample, the gesture with the shortest distance is the ADD gesture with 0.008, while the greatest distance is in the ABD gesture with 0.05. With regard to the STD, a small and consistent boundary circle indicates that the gesture is similar across the subject sample. For LH, the lowest mean STD is in the FIN group, with a mean of 0.01. The most consistent gesture is ADD while the EXT and ABD gestures have the highest SD of 0.06 and 0.08, respectively.

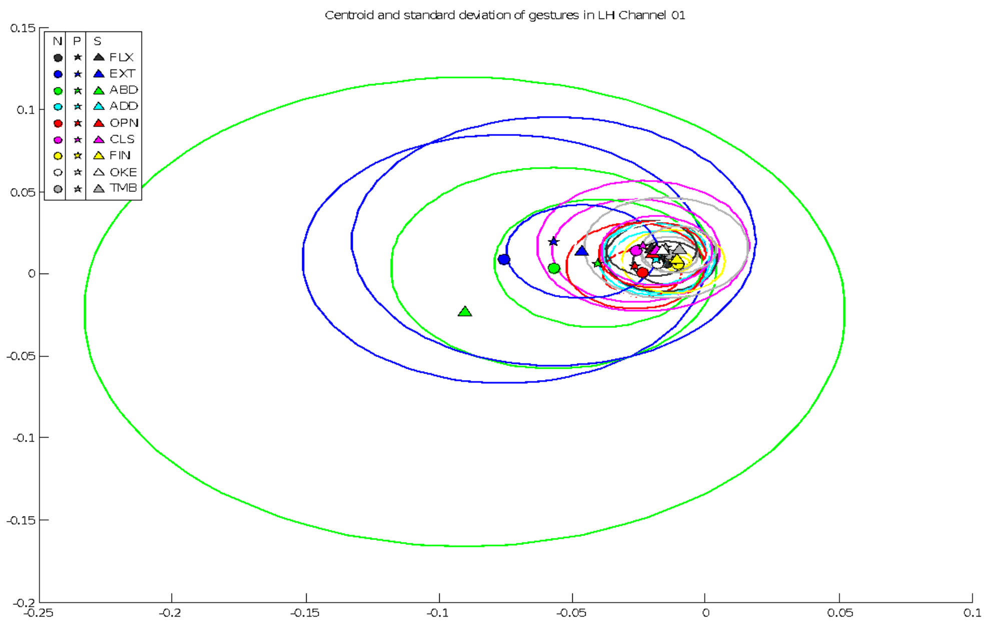

Figure 3: The scatter plot of FLX.LH.CH1 represented by the mean centroid (coordinate) and standard deviation (radius) of 20 subjects, displayed with the top 2 principal components. The plot shows that the centroid and its region overlaps with other gestures. A single channel does not capture enough EMG variation to classify all the nine gestures, hence, the overlaps of data.

2. Results of classification of pair-wise gestures over individual channels

To better represent the data, the gestures were re-rendered into a 9 x 9 scatter plot matrix, as shown in Figure 4 where the individual gestures are plotted in pairs. By placing the signals in pairs, e.g., FLX-EXT, FLX-ABD, FLX-ADD etc., there will be more room for cluster separation. The axes are PC1 (82%) and PC2 (9%), which weights in 91% of the variations.
The reconstructed scatter plot matrix of the gesture performed by subject F01 FLX.DN.LH shown here is divided into all possible gesture pairs. The first row shows the FLX against other gestures, while the second row features the EXT and so forth. The class separation is more evident now; the FLX-EXT pair shows good separation, which is consistent with previous results. Figure 5 renders the close up of the gesture pair FLX-EXT, which shows good separation and TMB-OKE which is poorly separated.
Generally, the wrist gestures have a better classification rate compared to finger gestures. Good A good classification rate of above 80% can be achieved between wrist gestures, wrist-finger gestures but not finger-finger gestures. Due to their low and indistinctive amplitude signals, the finger-finger gestures have a high error rate.

3. Effects of forearm rotation towards classification accuracy

Table 1 shows the top five classification results of the single-channel analysis. All possible gesture pairs were classified against each other, amounting to 81 gesture pairs per position per hand. Due to the number of results, only the five gesture pairs with the best results per channel are displayed. The colour scale represents the classification accuracy of the pair. The true positive classification rate ranges from 80% to 97.5%. This is an indicator by of how far two gestures are distinct in a channel.
The gestures in at the top of the list represent the best classifiable gesture pair. In CH1 of the left hand, the EXT gesture is highest for both hands in all positions with 10 counts of occurrence. This means the EXT gesture is significant against the other gestures i.e., OPN-EXT, EXT-FLX. Thereafter, CH2-CH6 does not exhibit any similarities between the two hands. For the left hand, CH2 to CH6 recorded OPN, FIN ABD, ADD, and FIN, while the right-hand registered FIN, EXT, EXT, FIN, FIN respectively.

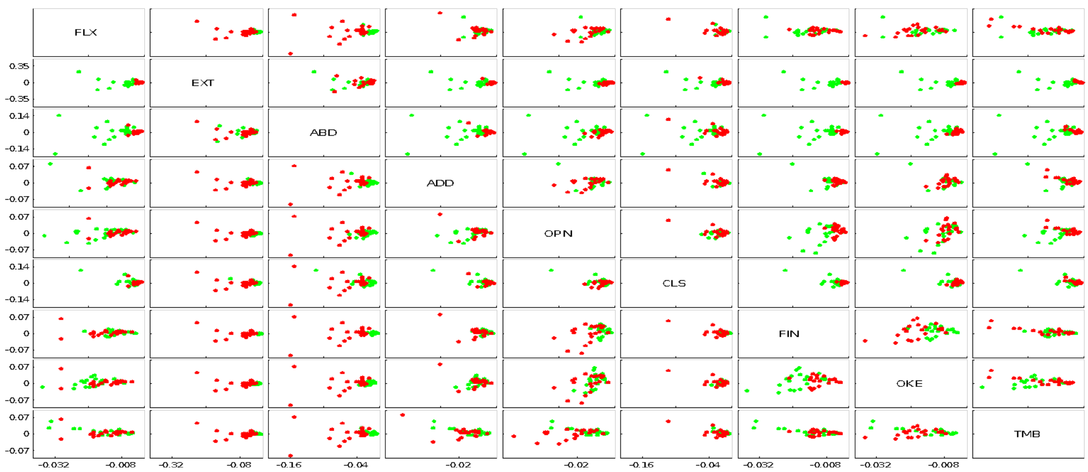

Figure 4: Scatter plot matrix sample of 20-subject LH CH1 separated by gestures. Red markers represent the Column element while the green elements represent the row

elements. Some of the gestures exhibit good separation, in this case, the FLX-EXT gesture pair. The plot axes show the first two principle components. Class separation is in fact higher because six principle components were used for classification.

Linear discriminant analysis (LDA) was applied to classify the signals, with the first six PCs. The results of classification for FLX-EXT and OKE-TMB gesture pairs are shown in Figure 5. A high classification rate will signify that the gestures and their signals are distinct. For instance, the FLX-EXT pair gesture scored an overall accuracy of 85% with 100% classification rate for FLX and 80% for EXT. However, the TMB–OKE gesture, the TMB gesture had a classification rate of 60% while the OKE gesture was 85%. As a result, the overall accuracy is 72.5%

By looking at the type of gesture pairs, the highest occurrence is the wrist-wrist gesture with 70 counts or 46% followed by wrist-finger (77 counts, 51%). The finger-finger gestures only constitute 3 counts (0.02%) to the results. Further observation also shows that the EXT gesture has the highest classification occurrence with a total of 77 counts followed by FIN (70) and ABD (54). The lowest attainable classification is the TMB with 21, followed by OKE with 23.

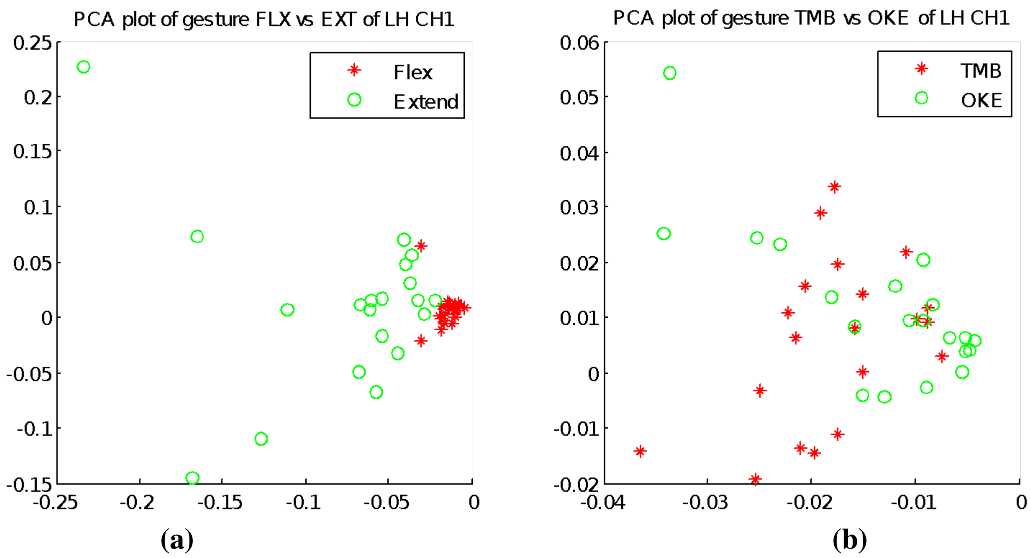

Figure 5: Close up PCA plot of (a) LH CH 1FLX-EXT, 85% c.a. and (b) TMB-OKE pair, 72.5% c.a. gestures. In general, the arm gestures have better separation compared to finger gestures. Gestures with better separation will result a higher classification rate.

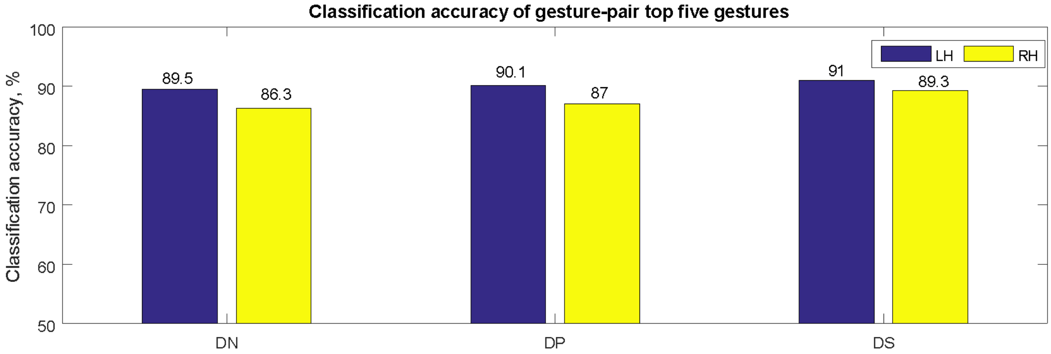

Figure 6: Effect of forearm rotation towards gesture-pair classification. Since there are only two classes, the classifier is able to predict the gestures accurately.

Table 1: Summary of multi-gesture classification, showing gestures with the highest classification accuracy per channel. This data suggests the most significant gesture obtainable from a certain channel.

		DN		DP		DS	
LH	CH1	FIN	70	FIN	70	FIN	60
	CH2	ABD	50	OKE	55	TMB	70
	CH3	EXT	55	FLX	55	FLX	60
	CH4	ABD	50	OPN	65	ABD	80
	CH5	FIN	70	ADD	75	ADD	70
	CH6	FIN	60	OPN	45	EXT	55
RH	CH1	FIN	60	FLX	60	EXT	55
	CH2	FIN	60	FIN	50	FIN	60
	CH3	EXT	70	FLX	65	FLX	65
	CH4	OPN	60	FLX	60	ABD	75
	CH5	ADD	60	ADD	55	ADD	65
	CH6	FIN	55	FIN	70	TMB	45

Table 12: Top five classified gesture pairs in all three positions for each channel, ranked by accuracy. The results show that the best classified gesture of the LH does not mirror to the RH. Generally, the wrist gestures have better classification rates compared to finger gestures.

DN											
LEFT HAND						RIGHT HAND					
CH1	CH2	CH3	CH4	CH5	CH6	CH1	CH2	CH3	CH4	CH5	CH6
OPN - EXT	OPN - ABD	FIN-EXT	AD D-ABD	AD D-ABD	OKE -FIN	CLS - EXT	FIN-EXT	AD D-EXT	EXT - FLX	FIN-EXT	FIN-EXT

EXT-FLX	CLS-OPN	OKE-FIN	OPN-ABD	FIN-ADD	OPN-ABD	OKE-EXT	OKE-EXT	CLS-EXT	ADD-EXT	FIN-ADD	FIN-ADD
ADD-EXT	FIN-ABD	OKE-FLX	FIN-ABD	OKE-ADD	FIN-ADD	EXT-FLX	FIN-FLX	FIN-FLX	OPN-EXT	FIN-CLS	FIN-OPN
FIN-EXT	OPN-FLX	OKE-ADD	FIN-ADD	TMB-ABD	FIN-EXT	FIN-EXT	CLS-EXT	OPN-FLX	CLS-EXT	ABD-EXT	FIN-CLS
OKE-EXT	OKE-FLX	TMB-ADD	TMB-FIN	ABD-FLX	FIN-ABD	FIN-ABD	TMB-EXT	EXT-FLX	FIN-FLX	OKE-ADD	ABD-EXT
DP											
LEFT HAND						RIGHT HAND					
CH1	CH2	CH3	CH4	CH5	CH6	CH1	CH2	CH3	CH4	CH5	CH6
EXT-FLX	CLS-FLX	FIN-OPN	FIN-ADD	ADD-ABD	FIN-EXT	TMB-EXT	FIN-FLX	TMB-FLX	EXT-FLX	FIN-EXT	FIN-EXT
ABD-EXT	FIN-FLX	CLS-EXT	ADD-ABD	OPN-ADD	EXT-FLX	EXT-FLX	CLS-FLX	EXT-FLX	ABD-FLX	FIN-ADD	FIN-OPN
CLS-EXT	OKE-FLX	FIN-EXT	TMB-ADD	FIN-ADD	CLS-OPN	ABD-FLX	OKE-EXT	OPN-FLX	CLS-EXT	OKE-ADD	EXT-FLX
TMB-EXT	TMB-FLX	OKE-OPN	ADD-EXT	OKE-ADD	ABD-EXT	ADD-EXT	TMB-EXT	OKE-FLX	TMB-FLX	TMB-FIN	ABD-EXT
FIN-EXT	ADD-FLX	EXT-FLX	OPN-EXT	ABD-EXT	TMB-EXT	FIN-EXT	FIN-EXT	CLS-FLX	FIN-FLX	ADD-ABD	FIN-ADD
DS											
LEFT HAND						RIGHT HAND					
CH1	CH2	CH3	CH4	CH5	CH6	CH1	CH2	CH3	CH4	CH5	CH6
FIN-EXT	FIN-EXT	FIN-FLX	ADD-ABD	ABD-FLX	OPN-FLX	FIN-ABD	FIN-FLX	CLS-EXT	ADD-ABD	ABD-EXT	FIN-EXT
TMB-FLX	OKE-FLX	FIN-EXT	OPN-ABD	ABD-EXT	FIN-OPN	FIN-EXT	TMB-EXT	EXT-FLX	CLS-ABD	FIN-EXT	ABD-EXT

CLS-EXT	OPN-EXT	TMB-ABD	FIN-OPN	ADD-ABD	EXT-FLX	ABD-FLX	TMB-FLX	ABD-FLX	ABD-FLX	FIN-ADD	OPN-FLX
TMB-EXT	TMB-FLX	TMB-FIN	TMB-ABD	FIN-FLX	FIN-EXT	CLS-EXT	FIN-EXT	ABD-EXT	FIN-CLS	ADD-ABD	FIN-ADD
TMB-CLS	TMB-FIN	TMB-EXT	OPN-EXT	FIN-EXT	CLS-EXT	TMB-EXT	OPN-FLX	CLS-FLX	OKE-CLS	OKE-ADD	TMB-FLX

Classification accuracy scale, in percent

100	97.5	95	92.5	90	87.5	85	82.5	80

Table 1: Summary of multi-gesture classification, showing gestures with the highest classification accuracy per channel. This data suggests the most significant gesture obtainable from a certain channel.

		DN		DP		DS	
LH	CH1	FIN	70	FIN	70	FIN	60
	CH2	ABD	50	OKE	55	TMB	70
	CH3	EXT	55	FLX	55	FLX	60
	CH4	ABD	50	OPN	65	ABD	80
	CH5	FIN	70	ADD	75	ADD	70
	CH6	FIN	60	OPN	45	EXT	55
RH	CH1	FIN	60	FLX	60	EXT	55
	CH2	FIN	60	FIN	50	FIN	60
	CH3	EXT	70	FLX	65	FLX	65
	CH4	OPN	60	FLX	60	ABD	75
	CH5	ADD	60	ADD	55	ADD	65
	CH6	FIN	55	FIN	70	TMB	45

The gesture pairs also do not match across the hands and position. For instance, the left hand CH6 top result pair is OKE-FIN (97.5%), while in place for the right hand is FIN-EXT (85%). The result across the table shows the same inconsistency. As a conclusion, there is no single channel which can significantly produce a gesture signal which is distinct enough to be associated with the respective channel. The analysis is advanced to determining the gesture pairs that retain classification rates when subjected to rotation. From the results, there are two observations: first, the top classification results change considerably with rotation. This suggests that rotation shifts the muscles beneath the electrodes and also, the EMG signals from the rotation are mixed with the signals of the gestures, which results a different EMG pattern. Next, the top classifiable EMG patterns are not the same for the two hands.

For every channel, the distance between the arm position markers signifies the variance of the signal. The closer the three markers mean the spread (variation) of the signal remains the same in spite of rotation. Ideally, the stems should be high and possess little variations in the arm rotation markers. There is no correlation between the results of the two hands. For LH, CH6 exhibits the most counts of low standard deviation (6 counts) while in RH, it is CH2 (7 counts).

A summary of the classification results of the top five gestures in Table 2 is shown in Figure 6. For a two-class gesture, the classifier can predict with excellent results, and accuracy change due to forearm rotation is negligible.

Table 2: Summary of multi-gesture classification, showing gestures with the highest classification accuracy per channel. This data suggests the most significant gesture obtainable from a certain channel.

		DN		DP		DS	
LH	CH1	FIN	70	FIN	70	FIN	60
	CH2	ABD	50	OKE	55	TMB	70
	CH3	EXT	55	FLX	55	FLX	60
	CH4	ABD	50	OPN	65	ABD	80
	CH5	FIN	70	ADD	75	ADD	70
	CH6	FIN	60	OPN	45	EXT	55
RH	CH1	FIN	60	FLX	60	EXT	55
	CH2	FIN	60	FIN	50	FIN	60
	CH3	EXT	70	FLX	65	FLX	65
	CH4	OPN	60	FLX	60	ABD	75
	CH5	ADD	60	ADD	55	ADD	65
	CH6	FIN	55	FIN	70	TMB	45

4. Classification of all nine gestures over a single channel

Figure 7 shows a summary of the classification results of all single channels. The classification results of both hands in all three positions are shown with the corresponding markers. As seen in the previous analysis, the DN-DP-DS gestures and the LH-RH gestures are unrelated in terms of classification accuracy. Generally, classification results are low, with an average of 34% and 30% for the LH and RH, respectively.

Table 2 shows the gesture with the highest classification accuracy for every channel. The FIN gesture dominates the table with five occurrences in the LH, ranging from 60%-70% and seven in the RH ranging from 55%-65%. Across the hands, only CH3 shows consistency of having the same gestures, namely EXT, FLX, FLX for the DN, DP and DS position. Across the rotations, the highest consistency can be observed at LH.CH1 with FIN (70%) while for RH.CH5 with ADD, 60% (mean).

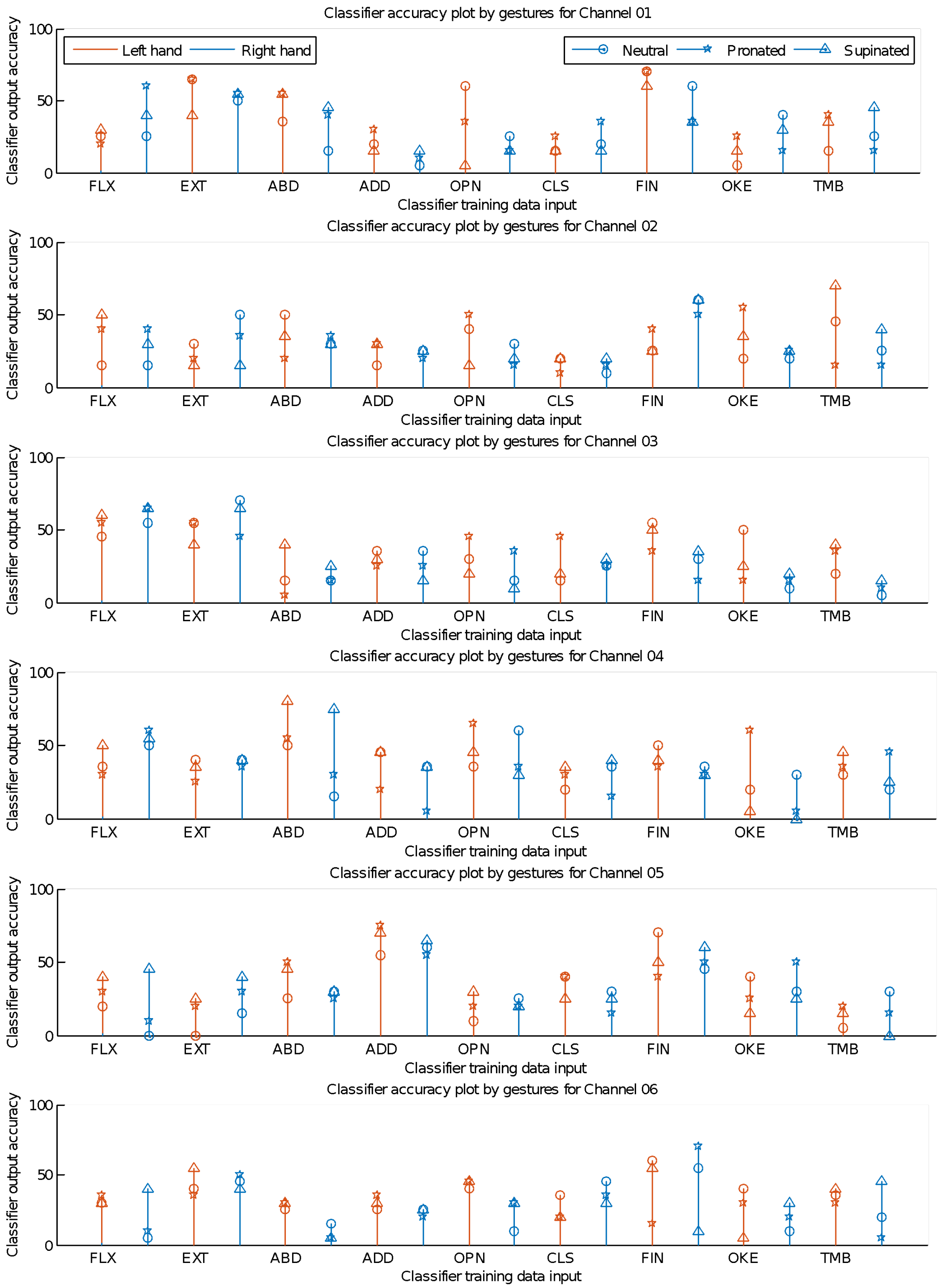

Figure 7: Effect of forearm rotation towards the classification of all nine gestures in one channel. A single channel cannot register enough pattern variations to accurately separate the gesture classes. In this case, the classification accuracy is

affected by rotation for some gestures, although the effect is not uniform-some gestures are more greatly affected than others.

The gesture pairs also do not match across the hands and position. For instance, the left hand CH6 top result pair is OKE-FIN (97.5%), while in place for the right hand is FIN-EXT (85%). The result across the table shows the same inconsistency. As a conclusion, there is no single channel which can significantly produce a gesture signal unique enough to be associated with. The analysis is advanced to determining the gesture pairs that retain classification rates when subjected to rotation. From the results, there are two observations: first, the top classification results change considerably with rotation. This suggests that rotation shifts the muscles beneath the electrodes and also, the EMG signals from the rotation are mixed with the signals of the gestures, which results a different EMG pattern. Next, the top classifiable EMG patterns are not the same for the two hands.

For every channel, the distance between the arm position markers signifies the variance of the signal. The closer the three markers, means the spread (variation) of the signal remains the same in spite of rotation. Ideally, the stems should be high and possess little variations in the arm rotation markers. There is no correlation between the results of the two hands. For LH, CH6 exhibits the most counts of low standard deviation (6 counts) while in RH, it is CH2 (7 counts). A summary of the classification results of the top five gestures in Table 2 are shown in Figure 6. For a two-class gesture, the classifier can predict with excellent results, and accuracy change due to forearm rotation is negligible.

5. Classification of all nine gestures over a single channel

Figure 7 shows a summary of the classification results of all single channels. The classification results of both hands in all three positions are shown with the corresponding markers. As seen in the previous analysis, the DN-DP-DS gestures and the LH-RH gestures are unrelated in terms of classification accuracy. Generally, classification results are low, with an average of 34% and 30% for the LH and RH, respectively.

Table 1 shows the gesture with the highest classification accuracy for every channel. The FIN gesture dominates the table with five occurrences in the LH, ranging from 60%-70% and seven in the RH ranging from 55%-65%. Across the hands, only CH3 shows consistency of having the same gestures, namely EXT, FLX, FLX for the DN, DP and DS position. Across the rotations, the highest consistency can be observed at LH.CH1 with FIN (70%) while for RH.CH5 with ADD, 60% (mean).

5. Limitations of Study and Its Implications

Gesture strength and timing was not strictly enforced. Subjects were free to perform the gestures in the manner they are comfortable with. As a result, the EMG variations that manifest are not only due to physiological differences, but also how the subject performed the gesture. As a remedial measure, care was taken when attaching the electrodes to ensure that variations due to electrode placements are minimized.

During recording, the nine gestures were performed in succession for each arm position. These gestures were manually spliced during post-processing. Therefore, the EMG variation due to neutral to pronation or supination movement was not accounted for in this study. Since the classification was performed offline, the wrist rotation signal can be ignored. However, in real-time classification, the wrist rotation should be included as a gesture.

6. Conclusions and Suggestions for Future Work

During the two-channel classification, good results of over 80% were attainable. However, with all gestures in the classifier, the results deteriorated to 30%. In this procedure, the single-channel analysis was performed to discover which signal is most classifiable per channel. First, for a pair of gestures, the classifier could clearly classify (above 90% accuracy rate) the wrist-wrist and wrist-finger gestures as opposed to the finger-finger gestures. However, when the classifier was introduced to all nine gestures, classification accuracy deteriorates due to the high amount of repetitive data.

Therefore, it has been established that accuracy of over 90% is achievable for subject independent, rotation independent gestures *if* there is only one pair of wrist-finger gesture involved.

We have shown that it is possible to classify wrist and finger gestures with common data pool. This is beneficial in practical application where retraining can be eliminated for various users. By limiting the number of gestures and selection of gestures, acceptable results are possible with a single set of training data.

We have also revealed that some gestures including the FIN, FLX and EXT retained a high classification accuracy across the rotation. This indicates that these signals do not change much when subjected to rotation. Normally a gesture in rotation requires separate training as different gestures. In the case of this study, the nine gestures in three arm positions will require three sets of training data. However, the result of our study indicates that a gesture in rotation can recognized as a single gesture. As a result, a single dataset of nine gestures in neutral position can be classified with test data from the pronation and supination positions. This will greatly further reduce training data as a gesture can be trained as a singular class for all three arm positions. The immediate benefits are a lighter computational burden: a reduced dataset enables a reduced setup time, and possibly faster and more accurate classification.

For future work, we recommend multi-channel classification, with training data from the neutral position used to classify test data from the pronation and supination position. The simultaneous multivariate data from six channel will provide improved separation between gestures and hence, higher classification accuracy.

Conclusion

It can be concluded with certainty that the nine gestures in neutral, pronation and supination must be treated as individual signals: this sums as 27 gestures per channel. During the two-channel classification, good results of over 80% were attainable. However, with all gestures in the classifier, results deteriorated to 30%. Furthermore, there is little correlation between the classification results, whether between hands or forearm rotation. The next process of the research would advance to assessing the signals collectively.

In this procedure, the single-channel analysis was performed to discover which signal is most classifiable per channel. First, for a pair of gestures, the classifier could clearly classify (above 90% accuracy rate) the wrist-wrist and wrist-finger gestures as opposed to the finger-finger gestures. However, when the classifier was introduced to all nine gestures, classification accuracy deteriorates due to the high amount of repetitive data.

Therefore, it has been established that accuracy of over 90% is achievable for subject independent, rotation independent gestures *if* there is only one pair of wrist-finger gesture involved.

Acknowledgement

This work was funded by the Malaysian Ministry of Education through the research grant—FRGS/2/2013/SG02/FKP/02/2/F00176.

References

Artemiadis P. (2012). EMG-based Robot Control Interfaces: Past, Present and Future. *Advances in Robotics & Automation*,**01**(02),10–12. http://www.omicsgroup.org/journals/2168-9695/2168-9695-1-e107.digital/2168-9695-1-e107.html

Cai S., Chen Y., Huang S., Wu Y., Zheng H., Li X., & Xie L. (2019). SVM-based classification of sEMG signals for upper-limb self-rehabilitation training. *Frontiers in Neurorobotics*, **13**.

Fougner A., Scheme E., Chan A. D. C., Englehart K., & Stavdahl Ø. (2011). Resolving the limb position effect in myoelectric pattern recognition. *IEEE Transactions on Neural Systems and Rehabilitation Engineering*, **19**(6), 644–651.

Fu Z., Bani Hashim A. Y., Jamaludin Z., & Mohamad I. S. (2016). Design of a low-cost EMG amplifier with discreet op-amps for machine control. *ARPN Journal of Engineering and Applied Sciences*, **11**(5), 3345–3349.

Fu Z., Bani Hashim A. Y., Jamaludin Z., Mohamad I. S., & Nasir N. (2017). Optimizing Surface Electromyography Acquisition without Right Leg Drive Circuit. *International Journal of Engineering Science Technologies*, **1**(1), 13–19.

Geng Y., Zhou P., & Li G. (2012). Toward attenuating the impact of arm positions on electromyography pattern-recognition based motion classification in transradial amputees. *Journal of NeuroEngineering and Rehabilitation*, **9**(1), 1–11.

Huang H., Zhang F., Sun Y. L., & He H. (2010). Design of a robust EMG sensing interface for pattern classification. *Journal of Neural Engineering*, **7**(5), 056005. http://stacks.iop.org/1741-2552/7/i=5/a=056005?key=crossref.3b85a946f7ea5624066a265f6d2f7b5b

Jiang N., Dosen S., Muller K. R., & Farina D. (2012). Myoelectric control of artificial limbsis there a need to change focus? [In the Spotlight]. In *IEEE Signal Processing Magazine* (Vol. 29, Issue 5, pp. 148–152).

Kerber F., Puhl M., & Krüger A. (2017). User-independent real-time hand gesture recognition based on surface electromyography. *Proceedings of the 19th International Conference on Human-Computer Interaction with Mobile Devices and Services, MobileHCI 2017*.

Khushaba R. N. (2014). Correlation analysis of electromyogram signals for multiuser myoelectric interfaces. *IEEE Transactions on Neural Systems and Rehabilitation Engineering*, **22**(4), 745–755.

Kim J., Mastnik S., & André E. (2008). EMG-based hand gesture recognition for realtime biosignal interfacing. *Proceedings of the 13th International Conference on Intelligent User Interfaces - IUI '08*, 30–39. http://portal.acm.org/citation.cfm?doid=1378773.1378778

Leijnse J.. N. A. L., Campbell-Kyureghyan N. H., Spektor D., & Quesada P. M. (2008). Assessment of individual finger muscle activity in the extensor digitorum communis by surface EMG. *Journal of Neurophysiology*, **100**(6), 3225–3235. http://jn.physiology.org/content/100/6/3225

Liu J., Zhang D., Jiang N., & Zhu X. (2015). Towards Zero Retraining for Myoelectric Control Based on Common Model Component Analysis. *IEEE Transactions on Neural Systems and Rehabilitation Engineering*, **24**(4), 1534–4320.

Mane S. M., Kambli R. A., Kazi F. S., & Singh N. M. (2015). Hand motion recognition from single channel surface EMG using wavelet & artificial neural network. *Procedia Computer Science*, **49**(1), 58–65. http://dx.doi.org/10.1016/j.procs.2015.04.227

Phinyomark A., Quaine F., Charbonnier S., Serviere C., Tarpin-Bernard F., & Laurillau Y. (2013). EMG feature evaluation for improving myoelectric pattern recognition robustness. *Expert Systems with Applications*, **40**(12), 4832–4840. http://dx.doi.org/10.1016/j.eswa.2013.02.023

Piskorowski J. (2013). Time-efficient removal of power-line noise from EMG signals using IIR notch filters with non-zero initial conditions. *Biocybernetics and Biomedical Engineering*, **33**(3), 171–178. http://dx.doi.org/10.1016/j.bbe.2013.07.006

Saponas T. S., Tan D. S., Morris D., Balakrishnan R., Turner J., & Landay J. A. (2009). Enabling always-available input with muscle-computer interfaces. *UIST 2009 - Proceedings of the 22nd Annual ACM Symposium on User Interface Software and Technology*, 167–176.

Sensinger J., Lock B. A., & Kuiken T. A. (2009). Adaptive Pattern Recognition of Myoelectric Signals: Exploration of Conceptual Framework and Practical Algorithms. *Chinese Journal of Applied Ecology*, **17**(3), 270–278.

Shenoy P., Miller K. J., Crawford B., & Rao R. N. (2008). Online electromyographic control of a robotic prosthesis. *IEEE Transactions on Bio-Medical Engineering*, **55**(3), 1128–1135.

http://www.ncbi.nlm.nih.gov/pubmed/18334405

Souissi H., Zory R., Bredin J., & Gerus P. (2017). Comparison of methodologies to assess muscle co-contraction during gait. *Journal of Biomechanics*, **57**, 141–145. http://dx.doi.org/10.1016/j.jbiomech.2017.03.029

Stival F., Michieletto S., & Pagello E. (2016). Online subject-independent modeling of sEMG signals for the motion of a single robot joint. *Proceedings of the IEEE RAS and EMBS International Conference on Biomedical Robotics and Biomechatronics*, **2016**-**July** 1110–1116.

Stoica A., Assad C., Wolf M., You K. S., Pavone M., Huntsberger T., & Iwashita Y. (2012). Using arm and hand gestures to command robots during stealth operations. *Multisensor, Multisource Information Fusion: Architectures,Algorithms,andApplications2012*,84070G1-84070G9. http://proceedings.spiedigitallibrary.org/proceeding.aspx?articleid=1354947

Sun B., & Chen W. (2012). Classification of SEMG Signals Using Integrated Neural Network with Small Sized Training Data. *Biomedical Engineering: Applications, Basis and Communications*, **24**(04), 365–376.

Watts P. B., Jensen R. L., Gannon E., Kobeinia R., Maynard J., & Sansom J. (2008). Forearm EMG During Rock Climbing Differs from EMG During Handgrip Dynamometry. *International Journal of Exercise Science*, **1**(1), 4–13. http://digitalcommons.wku.edu/ijes/vol1/iss1/2/

Xu Z., Xiang C., Yun L., Lantz V., Kong-Qiao W., & Yang J. (2011). A Framework for Hand Gesture Recognition Based on Accelerometer and EMG Sensors. *IEEE Transactions on Systems, Man, And Cybernetics—Part A: Systems and Humans*, **41**(6), 1064–1076.

Yang D., Yang W., Huang Q., & Liu H. (2017). Classification of Multiple Finger Motions during Dynamic Upper Limb Movements. *IEEE Journal of Biomedical and Health Informatics*, **21**(1), 134–141.

Yung M., & Wells R. P. (2013). Changes in muscle geometry during forearm pronation and supination and their relationships to EMG cross-correlation measures. *Journal of Electromyography and Kinesiology*, **23**(3), 664–672. http://dx.doi.org/10.1016/j.jelekin.2013.01.001